https://doi.org/10.5194/egusphere-2023-3125
Preprint. Discussion started: 8 January 2024
© Author(s) 2024. CC BY 4.0 License.

Diverse organic carbon dynamics captured by radiocarbon analysis of distinct compound classes in a grassland soil

Katherine E. Grant[1*], Marisa N. Repasch[1,2,3], Kari M. Finstad[1], Julia D. Kerr[1], Maxwell Marple[1], Christopher J. Larson[1,4], Taylor A. B. Broek[1,5], Jennifer Pett-Ridge[1,6], and Karis J. McFarlane[1]

[1]Physical and Life Sciences Directorate, Lawrence Livermore National Laboratory, Livermore, CA 94550, USA
[2]Institute of Arctic and Alpine Research, University of Colorado, Boulder, CO, USA
[3]Earth and Planetary Sciences, University of New Mexico, Albuquerque, NM, USA
[4]Department of Earth and Environmental Science, University of Pennsylvania, Philadelphia, PA, USA
[5]National Ocean Sciences Accelerator Mass Spectrometry (NOSAMS) Facility, Woods Hole Oceanographic Institution Woods Hole, MA, USA
[6]Life and Environmental Sciences Department, University of California-Merced, Merced, CA, USA

Correspondence to: Katherine E. Grant (grant39@llnl.gov)

Abstract. Soil organic carbon (SOC) is a large, dynamic reservoir composed of a complex mixture of plant and microbe derived compounds with a wide distribution of cycling timescales and mechanisms. The distinct residence times of individual C components within this reservoir depend on a combination of factors, including compound reactivity, mineral association, and climate conditions. To better constrain SOC dynamics, bulk radiocarbon measurements are commonly used to trace biosphere inputs into soils and estimate timescales of SOC cycling. However, understanding the mechanisms driving the persistence of organic compounds in bulk soil requires analyses of SOC pools that can be linked to plant sources and microbial transformation processes. Here, we adapt approaches, previously developed for marine sediments, to isolate organic compound classes from soils for radiocarbon (^{14}C) analysis. We apply these methods to a soil profile from an annual grassland in Hopland, California (USA) to assess changes in SOC persistence with depth to 1 m. We measured the radiocarbon values of water extractable organic carbon (WEOC), total lipid extracts (TLE), total hydrolysable amino acids (AA), and an acid-insoluble (AI) fraction from bulk and physically separated size fractions (<2 mm, 2 mm–63 μm, and <63 μm). Our results show that $\Delta^{14}C$ values of bulk soil, size fractions, and extracted compound classes became more depleted with depth, and individual SOC components have distinct age-depth distributions that suggest distinguishable cycling rates. We found that AA and TLE cycle faster than the bulk soils and the AI fraction. The AI was the most ^{14}C depleted fraction, indicating it is the most chemically inert in this soil. Our approach enables the isolation and measurement of SOC fractions that separate functionally distinct SOC pools that can cycle relatively quickly (e.g., plant and microbial residues) from more passive or inert SOC pools (associated with minerals or petrogenic) from bulk soils and soil physical fractions. With the effort to move beyond SOC bulk analysis, we find that compound class ^{14}C analysis can improve our understanding of SOC cycling and disentangle the physical and chemical factors driving OC cycling rates and persistence.

https://doi.org/10.5194/egusphere-2023-3125
Preprint. Discussion started: 8 January 2024
© Author(s) 2024. CC BY 4.0 License.

1 Introduction

Soil organic carbon (SOC) is a large and complex terrestrial reservoir of Earth's organic carbon (OC) (Jobbágy and Jackson, 2000). It is a highly dynamic and open pool with inputs from decaying plant material, living roots, and soil microbes, and with losses driven by microbial activity that includes the degradation and transformation of compounds (Angst et al., 2021). The results of these processes is a heterogenous mixture of organic compounds with different radiocarbon (^{14}C) ages and reactivities (Lehmann and Kleber, 2015; Shi et al., 2020; Trumbore and Harden, 1997; Gaudinski et al., 2000; Mcfarlane et al., 2013). This complexity obscures the mechanisms that control overall OC persistence in soils, resulting in a continued debate over the degree to which environmental factors, physical protection, and chemical composition influence SOC reactivity and persistence (Lützow et al., 2006; Lehmann et al., 2020; Schmidt et al., 2011).

Bulk analysis methods have not fully demonstrated how physical protection and chemical composition interact to influence SOC persistence, and so novel organic matter characterization methods are necessary to shed light on how different compound classes of OC are preserved in soils and through what mechanisms. For example, we need to understand how the chemical structure of OC influences interactions with mineral surfaces, such as aggregation or sorption, as well as how the environment influences the decomposition and resource availability of certain OC compounds and functional groups. However, it has been difficult to isolate, identify, and quantify pools of OC that directly link to in-situ OC chemical compounds (Von Lutzow et al., 2007). Therefore, multiple approaches are needed to fully understand the interplay between chemical compound persistence and mineral interaction functions in soil.

One approach used to investigate the controls on SOC persistence is to separate soil into operationally defined carbon pools (e.g., size or density fractions) and characterize the resulting fractions. This approach has demonstrated that association of OC with soil minerals is a critical mechanism for C stabilization (Vogel et al., 2014; Mikutta et al., 2007), as ^{14}C data indicate that some mineral-associated C can persist for thousands of years (Torn et al., 2009). However, ^{13}C labelling experiments show that some mineral-associated C cycles quickly, within months to years (Keiluweit et al., 2015; De Troyer et al., 2011). Likely, some biomolecules form strong associations with mineral surfaces, such as long-chain lipids with iron oxides (Grant et al., 2022), while other compounds only loosely associate with minerals (e.g., through hydrophobic interactions with other OC compounds) (Kleber et al., 2007). Therefore, mineral-associated OC isolated using soil physical fractionation methods remains a heterogenous mixture of OC molecules that have a distribution of turnover times, rather than a homogenous and intrinsically stable SOC pool (Stoner et al., 2023; Van Der Voort et al., 2017).

Another approach that can yield finer resolution of OC turnover than traditional techniques is to isolate and measure the isotopic signature of specific compounds (Von Lutzow et al., 2007). In marine and riverine systems, compound specific radiocarbon analysis (CSRA) has been used monitor the degradation of organic carbon through the marine water column (Loh et al., 2004), characterize marine particulate OC (Hwang and Druffel, 2003), constrain terrestrial OC burial and export from river systems (Galy et al., 2015; Galy et al., 2008; Repasch et al., 2021), and determine effect of OC export and burial on precipitation patterns and climate (Hein et al., 2020; Eglinton et al., 2021). Different types of compounds including plant or

https://doi.org/10.5194/egusphere-2023-3125
Preprint. Discussion started: 8 January 2024
© Author(s) 2024. CC BY 4.0 License.

microbial lipid biomarkers (Douglas et al., 2018; Huang et al., 1996), amino acids (Bour et al., 2016; Blattmann et al., 2020), lignin (Feng et al., 2017; Feng et al., 2013), certain carbohydrate compounds (Kuzyakov et al., 2014; Gleixner, 2013), and pyrogenic carbon (Coppola et al., 2018) can be isolated and analysed for ^{14}C leading to a more detailed understanding of the cycling of targeted compounds in the environment. Each of these specific compounds can provide information related to the persistence and/or source of the OC in soils. For instance, lipids are found in plant cell walls and microbial cell membranes and used for energy storage. Amino acids are necessary for protein formation and enriched in nitrogen (N) relative to other plant and microbial residues. These two compound classes not only have diverse chemical reactivities which allows for insight into chemical compound persistence. Understanding the abundance and age of these two biomarkers in soils can help differentiate the source of C used by soil microbes for metabolism and growth (e.g., new C inputs vs older, recycled soil C) as well as the transformation pathways that yield persistent SOC.

Recently, CSRA approaches developed for these environments have been applied to soil showing promise for identifying distinct ages of plant and microbial biomarkers in SOC (Gies et al., 2021; Grant et al., 2022; Van Der Voort et al., 2017; Jia et al., 2023; Douglas et al., 2018). Most of these CSRA studies applied to SOC have targeted specific, individual biomarkers in soils, which generally contribute less than 5% of the entire carbon pool (Lützow et al., 2006; Kögel-Knabner, 2002). This approach can be can be too specific to elucidate wholistic mechanisms for SOC persistence and turnover that pertain to the majority of SOC. While individual biomarker ages, such as single ages of a particular lipid or single amino acid, can be useful in some contexts, comprehensive understanding carbon compound class persistence is vital for understanding and modelling the soil carbon reservoir's vulnerability to degradation.

To strike a balance between too specific and too broad, some researchers have characterized broader compound classes rather than isolating a single biomarker. For example, this ^{14}C-compound class approach has been applied to marine dissolved and particulate OC with a range of compounds, such as total lipids and total amino acids, to provide a broader understanding of OC persistence in oceans (Wang et al., 2006; Wang et al., 1998; Loh et al., 2004). Wang et al. (1998) established a sequential extraction procedure to analyse ^{14}C abundance of total lipids, amino acids, carbohydrates, and a residual acid insoluble fraction from marine POC and sediments. This approach yielded distinct differences in ^{14}C age and abundance of the amino acids, lipids, and the acid insoluble fraction in POC from the marine water column and sediment, as well as in costal verses open ocean environments. Loh et al. (2004) found the lipid fraction of dissolved OC and POC to be the oldest fraction measured in both the Atlantic and Pacific oceans, while the acid insoluble fraction was intermediate in age, and the amino acids and carbohydrates contained a significant contribution of modern carbon. Wang and Druffel (2001) also used this approach and found that the lipids were the oldest compound class from sediments in the Southern Ocean, but the acid insoluble residue was very similar in age to the lipid fraction. These studies suggest that compound classes can have independent cycling rates, but these cycling rates can be influenced by OC environment.

Here, we apply a ^{14}C compound class approach to soils to more broadly understand SOC turnover mechanisms. We characterize the distribution and ^{14}C age of multiple SOC pools with depth in a well-studied Californian grassland, using soil physical fractionation (Mcfarlane et al., 2013; Poeplau et al., 2018) and modified compound class extraction methods

https://doi.org/10.5194/egusphere-2023-3125
Preprint. Discussion started: 8 January 2024
© Author(s) 2024. CC BY 4.0 License.

previously detailed for marine sediments (Wang et al., 1998). We measured the radiocarbon values of water extractable organic carbon (WEOC), total lipid extracts (TLE), total hydrolysable amino acids (AA), and an acid-insoluble (AI) fraction from bulk and physically separated size fractions (bulk soil, sand, and silt+clay). We expected the TLE to be older than its source fraction (bulk soil, sand, or silt+clay), to be older with depth as the decline in plant inputs necessitates recycling and use of older SOC, and to be older in the silt+clay fraction as its high surface area should result mineral-OC associations that protect SOC from soil microbes. We expected the AA to cycle faster than the TLE fraction and the bulk SOC pool based on the young ^{14}C ages found for AA extracted from in marine sediments (Wang et al., 1998; Wang and Druffel, 2001), but hypothesized that recycling of amino acids at depth by soil microbes might result in an increase in the age of AA below 50 cm. Finally, we expected AI to have old C, similar to the TLE, as seen found in marine sediments (Wang et al., 1998). Here, we describe the relative abundance and radiocarbon content of total lipid and amino acid compound class extracts and compare carbon storage and cycling rates within physical soil size fractions. These data provide a foundation for the continued application of compound class ^{14}C work to the understanding and modelling of soil OC persistence.

2 Materials and Methods

2.1 Site and Sample Description

Soil samples were collected from the University of California's Hopland Research and Extension Center (HREC) in January 2022. The site is an annual grassland with a Mediterranean-type climate; mean annual precipitation (MAP) averages 940 mm per year and the mean annual temperature is 15˚C (Nuccio et al., 2016). The underlying geology consists of mixed sedimentary rock of the Franciscan formation. The soils are designated Typic Haploxeralfs of the Witherall-Squawrock complex (Soil Survey Staff, 2020). The samples were collected from the "Buck" site (39.001º, -123.069º) where the vegetation is dominated by annual wild oat grass, *Avena barbata* (Kotanen, 2004; Bartolome et al., 2007). Soils were collected from a freshly dug soil pit at four depths: 0–10 cm, 10–20 cm, 20–50 cm, and 50–100 cm. Samples were stored in sealed plastic bags at ambient temperature and transported to the laboratory in Livermore, CA. Soil samples were air dried, homogenized, and sieved to 2 mm, with the >2 mm fraction retained for further analysis. Samples were subdivided for soil characterization, physical size separations, chemical compound extractions, and density fractionation.

2.2 Physical Fractionation

To compare compound classes between mineral-associated OC and mineral-free OC, we used a salt-free and chemical-free method for isolating the mineral-associated organic matter from the free particulate organic matter (Fig. 1a). Under the assumption that mineral-associated carbon is primarily found in the silt+clay (<63 μm) particle size fraction, we used a size fractionation sieving method where air-dried samples were dry-sieved into three size fractions: bulk soil (<2 mm), sand (2 mm - 63 μm), and silt+clay (<63 μm) (Lavallee et al., 2020; Poeplau et al., 2018). Additionally, because the majority of free particulate organic carbon (POC) is contained in the sand faction, we used a "water density" separation to remove the low

https://doi.org/10.5194/egusphere-2023-3125
Preprint. Discussion started: 8 January 2024
© Author(s) 2024. CC BY 4.0 License.

density POC from the mineral matter in this fraction, resulting in a POC (<1g mL^{-1}) fraction and a POC-free (>1g mL^{-1}) sand faction.

To further characterize these soils and aid in interpretation of our data, we compared the size fractionated samples to samples separated by density using sodium polytungstate (SPT-0 adjusted to a density of 1.65 g ml^{-1}) (Poeplau et al., 2018) (see SI Section 1.1 for detailed methods). We chose to focus our compound class extraction efforts on size fractionated samples to avoid chemical alteration of SOC during exposure to SPT.

To constrain any contributions of parent materials to SOC, we processed and analyzed the rock fraction (> 2mm) (Agnelli et al., 2002; Trumbore and Zheng, 1996). Rocks were washed with 18.2 MΩ water in an ultrasonic bath to remove surface contamination, rinsed with 1N HCl to remove any additional weathered material loosely adhered to the surface, dried at 60°C, then manually crushed.

A large, representative aliquot (~10 g) of the bulk and each physical fraction were ball milled and measured for total organic carbon (TOC, wt %), C/N ratio, $\delta^{13}C$ and $\Delta^{14}C$ (Section 2.6). In addition, we analyzed the bulk soils at each depth with nuclear magnetic resonance (^{13}C NMR) to assess the broad structural complexity of the OC in the bulk soil (SI Section 2).

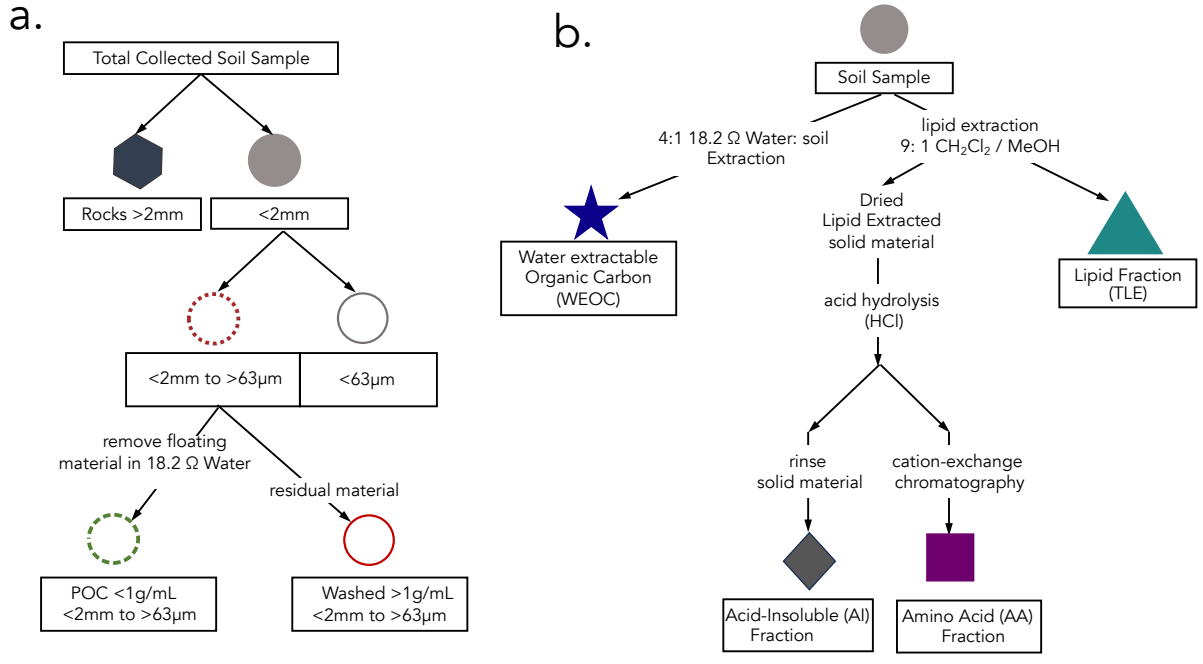

Figure 1: Schematics of protocols used in this study for a) fractionation by size and b) extraction of targeted compound classes.

2.3 Water-extractable organic carbon (WEOC)

https://doi.org/10.5194/egusphere-2023-3125
Preprint. Discussion started: 8 January 2024
© Author(s) 2024. CC BY 4.0 License.

The water-extractable organic carbon (WEOC) fraction was collected from 80 g of bulk soil with 18.2 MΩ water using a 4:1 water to soil ratio (Van Der Voort et al., 2019; Lechleitner et al., 2016; Hagedorn et al., 2004). Saturated soil samples were shaken for 1 hour and then filtered through a pre-rinsed 0.45 µm polyethersulfone (PES) Supor filter under vacuum. An aliquot was taken for dissolved organic carbon (DOC) measurement on a Shimadzu TOC-L combustion catalytic oxidation instrument. Sample concentrations were determined using a nine-point DOC calibration curve ranging from 0-200 mgC L^{-1}. The WEOC fraction was dried using a Labconco CentriVap centrifugal drying system at 40°C and subsequently transferred with 0.1N HCl into pre-combusted quartz tubes to eliminate any inorganic carbon dissolved in the aqueous fraction. The acidified WEOC fractions were then dried down using the CentriVap. Dried samples were flame sealed under vacuum (Section 2.6) for subsequent carbon isotope analyses.

2.4 Total Lipid Extraction (TLE)

Total lipids (TLE) were extracted from the soil samples using an Accelerated Solvent Extraction (ASE) system (Dionex 350, Thermo Scientific) in duplicate. The TLE was extracted from the bulk, sand, silt+clay, and the dense fraction (> 1.65 g ml^{-1}; DF). An aliquot of 10–30 g of soil was loaded into an a stainless-steel ASE extraction cell depending on TOC content (Rethemeyer et al., 2004). The ASE was set to extract the sample for 5 minutes with a holding temperature of 100°C at 1500 PSI. Lipids were extracted using a 9:1 ratio of dichloromethane (DCM or syn: methylene chloride) to methanol (Wang et al., 1998; Van Der Voort et al., 2017; Grant et al., 2022). The TLE was dried under constant ultra-pure N_2 flow at 40°C using a nitrogen dryer (Organomation Multivap Nitrogen Evaporator). The TLE was resuspended in ~5ml of 9:1 DCM:Methanol then transferred to pre-combusted quartz tubes, dried again, and analyzed for ^{14}C as described below (Section 2.5). Total CO_2 produced by the combustion of the TLE was measured manometrically on the ^{14}C vacuum lines during graphitization. Process blank samples were analyzed with each batch (SI Section 3.1).

2.5 Amino Acid (AA) Extraction

Amino acids (AA) were extracted from the lipid-extracted residual bulk and silt+clay size fraction with an acid hydrolysis procedure, desalted, and isolated with cation exchange chromatography using methods modified from those used in marine systems (Wang et al., 1998; Ishikawa et al., 2018; Blattmann et al., 2020). Briefly, a 500 mg soil aliquot was hydrolyzed with 6N HCl (ACS grade) under an N_2 atmosphere for 19-24 hours at 110°C. After hydrolysis, amino acids in solution were separated from the solid acid insoluble (AI) fraction via centrifugation for 5 minutes at 2500 rpm. The AI fraction was subsequently washed at a minimum three additional times with 0.2N HCl to ensure complete AA recovery. The supernatant was collected in a single pre-combusted vial and then filtered through a pre-combusted quartz wool fiber plug to remove extraneous sediment particles. The filtered hydrolysate was dried using a CentriVap at 60°C for 4 hours. The dried supernatant was redissolved in 1 ml 0.1N HCl and loaded onto a preconditioned resin column (BioRad 50WX8 200-400 mesh resin) to isolate the AA from other hydrolyzed organic matter and remove excess chloride. Details of the procedure can be found in Ishikawa et al., 2018. Briefly, once the sample was loaded on the column, it was rinsed with three bed volumes (~6 ml) of 18.2

https://doi.org/10.5194/egusphere-2023-3125
Preprint. Discussion started: 8 January 2024
© Author(s) 2024. CC BY 4.0 License.

MΩ H_2O. The free AA were eluted with 10 ml of 2N ammonium hydroxide (NH_4OH), then transferred into pre-baked quartz tubes, dried at 60°C in the CentriVap, and finally sealed and combusted for isotopic analysis. The remaining rinsed solid residual after hydrolysis is the acid-insoluble (AI) fraction. These are processes as a solid sample for isotopic analysis.

2.6 Isotopic and elemental analysis

All samples were analyzed for radiocarbon (^{14}C) at the Center for Accelerator Mass Spectrometry (CAMS) at Lawrence Livermore National Lab (LLNL) in Livermore, California. Samples were either measured on a 10 MV Van de Graaf FN or 1MV NEC Compact accelerator mass spectrometer (AMS) (Broek et al., 2021), with average errors of $F^{14}C = 0.0035$. For solid soil analysis, 10 to 250 mg of ground material was weighed into a pre-combusted quartz tubes along with 200 mg CuO and Ag, flame sealed under vacuum, then combusted at 900°C for 5 hours. The CO_2 was reduced to graphite on preconditioned iron powder under H_2 at 570°C (Vogel et al., 1984). Measured ^{14}C values were corrected using $\delta^{13}C$ values and are reported as age-corrected $\Delta^{14}C$ values using the following the conventions of Stuiver and Polach (1977). Extraneous C was quantified for the TLE and AA extractions (SI Table 4 and SI Section 3). For ease of reference, we included conventional radiocarbon ages in our figures and tables. We quantified turnover times using the single pool turnover model described in Sierra et al. (2014) and Van Der Voort et al. (2019) and explained in detail in Trumbore (2000) and Torn et al. (2009). This approach generates two solutions for pools with $\Delta^{14}C > 0$ ‰, one corresponding to each side of the atmospheric ^{14}C-CO_2 curve over the last 70 years (Hua et al., 2022). Unfortunately, we cannot identify the correct solution (Mcfarlane et al., 2013; Trumbore, 2000), especially for TLE and AA fractions from the top 20 cm, as we do not have multiple time points or additional constraints such as pool-specific input or decomposition rates. Therefore, our data analysis and interpretations rely on the reported $\Delta^{14}C$ values. All individual ^{14}C measurements used in this study are listed in the Supplementary Information (SI Table 1 and 2).
For each solid sample, a dried homogenized aliquot was analyzed for TOC concentration and $\delta^{13}C$ using an elemental analyzer (CHNOS) coupled to an IsoPrime 100 isotope ratio mass spectrometer at the Center for Stable Isotope Biogeochemistry (CSIB) at the University of California, Berkeley. Samples are assumed to have no inorganic carbon based on acid leaching tests and previously published ^{14}C work at this site (Finstad et al, 2023, Foley et al., 2023). $\delta^{13}C$ was measured in duplicate for each solid sample and errors represent the standard deviation of the mean. $\delta^{13}C$ values of WEOC, TLE, and AA extracts were measured on a split of the cryogenically purified CO_2 and were analyzed at the Stable Isotope Geosciences Facility at Texas A&M University on a Thermo Scientific MAT 253 Dual Inlet Stable Isotope Ratio Mass Spectrometer (SI Table 1).

2.7 Data analysis

Data was analyzed using MATLAB version R20223 and R v. 3.614 (R Core Team, 2019). Linear regressions were calculated between the sample depth mid-point and $\Delta^{14}C$ values from both the size fractions as well as the extracted compounds (WEOC, TLE, AA, AI) from the different size fractions. This was done to directly compare the difference in $\Delta^{14}C$ value between the compound classes. Correlation coefficients, p-values and r^2 are provided in SI Table 3. Analysis of Variance (ANOVA) was used to assess differences in $\Delta^{14}C$ with depth, between TLE and AA, and between soil fractions. ANOVA tests were performed

https://doi.org/10.5194/egusphere-2023-3125
Preprint. Discussion started: 8 January 2024
© Author(s) 2024. CC BY 4.0 License.

in R v. 3.614 (R Core Team, 2019). In the text, results are reported as means followed by one standard error when n = 2 or 3 or by analytical error when n = 1.

3 Results

3.1 Radiocarbon values and characterization of the physical fractions

We used soil size and density fractionation to separate the bulk soil into fractions with different degrees of mineral protection. Radiocarbon content for the bulk soil, sand, and silt+clay (SI Table S3) became more ^{14}C depleted (older) with increasing depth (Table 1, Fig. 2). SOC in the silt+clay was consistently younger than in the bulk soil, with the average difference in $\Delta^{14}C$ values increasing from 4‰ at the surface to 87‰ at depth.

227

228 **Table 1. Carbon concentrations, mass fractions, and radiocarbon values for the size separations from the Buck Pit**

	bulk (<2mm)		sand-sized (2mm to 63µm)							silt+clay (<63µm)		
						POC-free >1g mL^{-1}		POC <1 gmL^{-1}				
Depth	%OC	$\Delta^{14}C \pm$ err (‰)	*mass f*	%OC	$\Delta^{14}C \pm$ err (‰)	%OC	$\Delta^{14}C \pm$ err (‰)	%OC	$\Delta^{14}C \pm$ err (‰)	*mass f*	%OC	$\Delta^{14}C \pm$ err (‰)
0-10 cm	3.14	31 ± 3	0.71	2.68	25 ± 3	2.08	25 ± 3	25.69	19 ± 3	0.29	4.25	34 ± 3
10-20 cm	1.22	-22 ± 3	0.69	0.94	-38 ± 3	0.77	-35 ± 3	25.99	-5 ± 3	0.31	1.84	-13 ± 3
20-50 cm	0.50	-116 ± 3	0.75	0.39	-142 ± 3	0.38	-149 ± 2	n.m.	4 ± 3	0.25	0.85	-79 ± 3
50-100 cm	0.25	-468 ± 3	0.79	0.23	-496 ± 3	0.18	-510 ± 2	n.m.	-10 ± 3	0.21	0.35	-380 ± 3

229

https://doi.org/10.5194/egusphere-2023-3125
Preprint. Discussion started: 8 January 2024
© Author(s) 2024. CC BY 4.0 License.

https://doi.org/10.5194/egusphere-2023-3125
Preprint. Discussion started: 8 January 2024
© Author(s) 2024. CC BY 4.0 License.

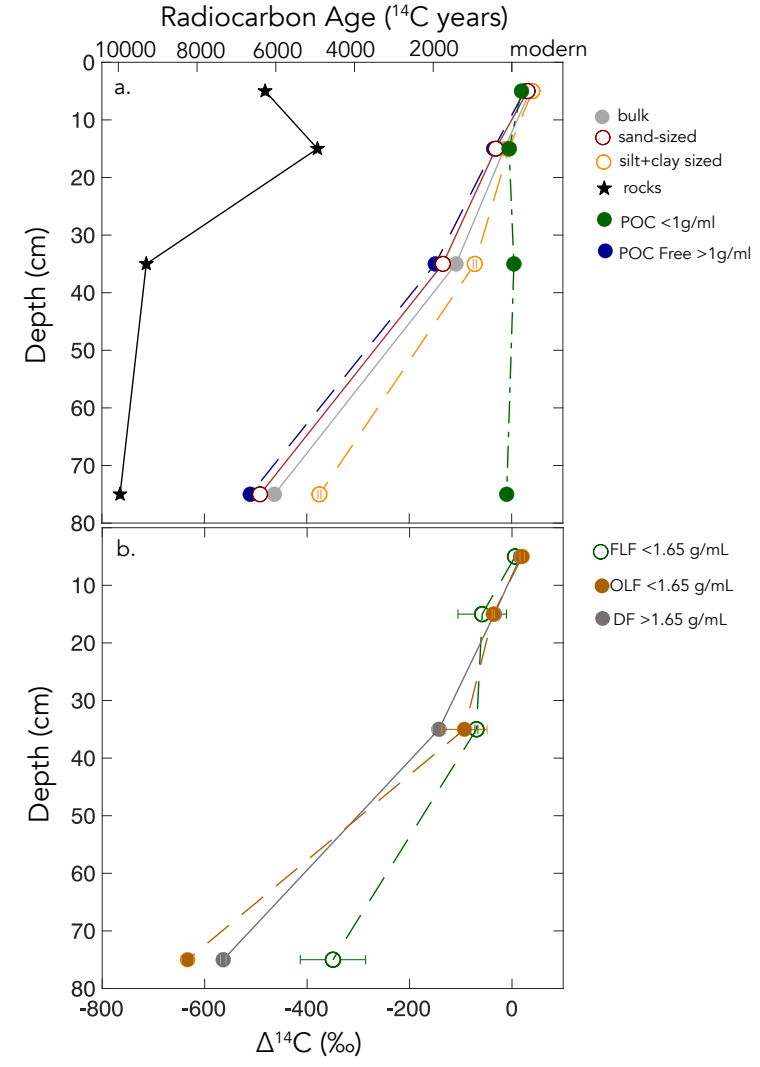

Figure 2: Δ^{14}C values by depth for a) size-fractions and b) density-fractions from the Buck soil pit. Conventional ^{14}C ages are provided for reference.

In the sand fraction, the Δ^{14}C values of POC were consistently near current atmospheric values (2 ± 3‰) and were not significantly correlated with depth. In contrast, the Δ^{14}C values of the POC-free sand-sized fraction declined with depth (+25 ± 3‰ to -510 ± 2‰, p = 0.006) and were indistinguishable from the POC-free sand fraction (Fig. 2). Density fractionation of the bulk soil resulted in most of the sample mass (> 98%) and OC (75–83%) recovered in the DF at all depths (SI Fig. S2).

https://doi.org/10.5194/egusphere-2023-3125
Preprint. Discussion started: 8 January 2024
© Author(s) 2024. CC BY 4.0 License.

3.2 Compound Class results from bulk soil and silt+clay

In both the bulk soil and silt+clay fraction, the extracted compound classes became ^{14}C-depleted with depth except for the WEOC, which had ^{14}C values that reflected C inputs recently fixed from the atmosphere throughout the soil profile (Fig. 2; SI tables). The $\Delta^{14}C$ values of the WEOC ranged from +14 ± 4‰ at the surface to -46 ± 4‰ at depth, and the DOC concentrations ranged from 43.2 to 6.7 mg C g soil^{-1} at the surface and at depth, respectively.

The TLE from the bulk soil had $\Delta^{14}C$ values that range from 17 ± 27 to -208 ± 6‰ (n = 2; ± SE) in the surface and deepest sample, respectively. In comparison, the TLE from the silt+clay fraction was modern at the surface and became more ^{14}C depleted with depth ($p < 0.001$), from +46 ± 4 to -204 ± 36 ‰. The slopes of the linear regressions of $\Delta^{14}C$ with depth were indistinguishable in TLE from the bulk soil and silt+clay. In addition, the TLE from the bulk TLE and silt+clay fraction TLE (SI Tables) had very similar $\Delta^{14}C$ values, but the bulk soil had less lipid-C extracted during each experiment (280 µg g C^{-1} in the 0-10 cm vs. 150 µg g C^{-1}; SI Table 2).

The $\Delta^{14}C$ values of the AA extracted from the bulk soil ranged from 54 ± 5 to -183 ± 24 (n = 2, SE) with depth (Fig. 3, SI Table S3). Similarly, the $\Delta^{14}C$ value of the AA fraction extracted from silt+clay declined with depth from +60 ± 3‰ (n = 2, SE) at the surface to -106 ± 4 ‰ (n = 2, SE) at 50-100 cm depth. The slopes of the AA extracted from the bulk and silt+clay-size fractions were statistically different, indicating that the AA extracted from the bulk soil became more depleted with depth than that extracted from the silt+clay (SI Table S3). Furthermore, AA fractions were enriched in ^{14}C values relative to the TLE or AI fraction ($p < 0.01$ for bulk soil and $p < 0.05$ for silt+clay).

The AI fraction was the oldest fraction found in our study at each depth. The $\Delta^{14}C$ values of the AI fraction ranged from -5± 2‰ to -633± 2‰ (analytical error, n=1) and declined with depth ($p < 0.01$ for bulk soil and silt+clay; Fig. 3; SI Table S3).

https://doi.org/10.5194/egusphere-2023-3125
Preprint. Discussion started: 8 January 2024
© Author(s) 2024. CC BY 4.0 License.

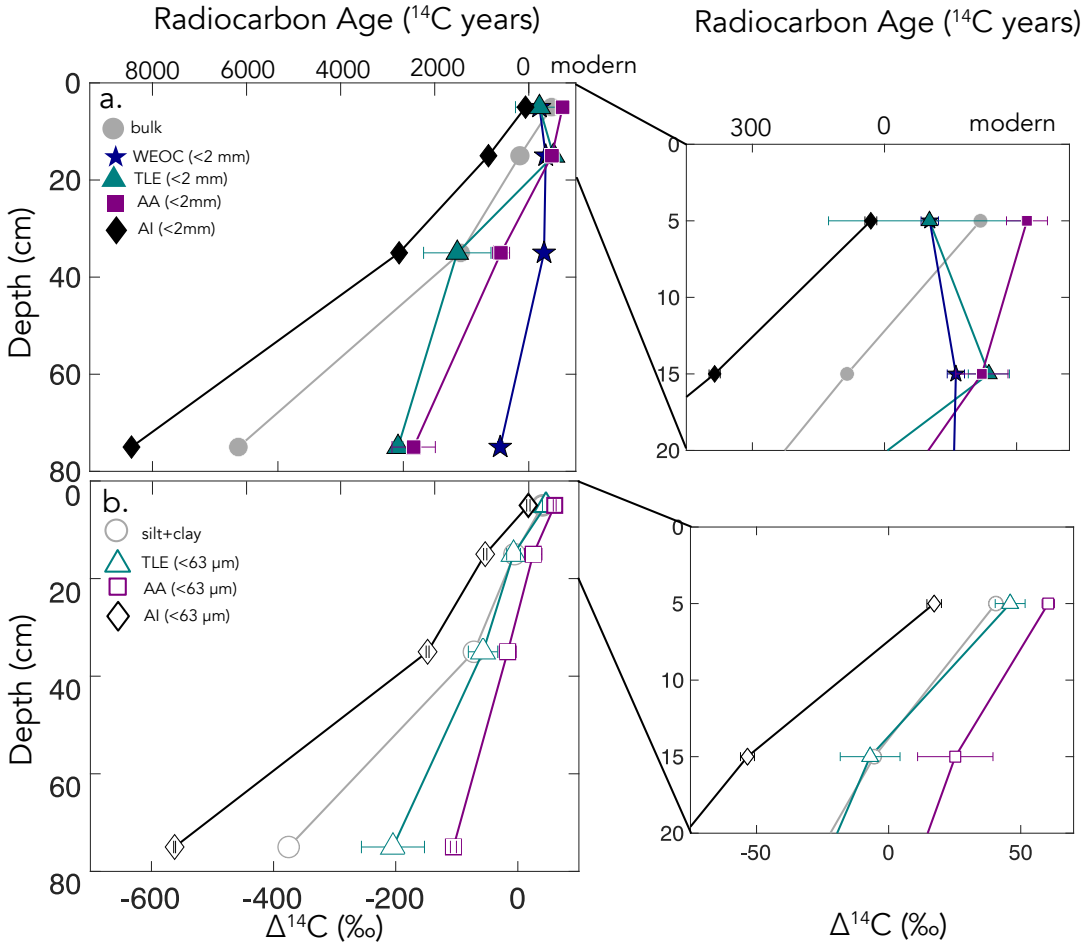

Figure 3: Δ^{14}C by depth for a) bulk soil and four compound class fractions extracted from bulk soil for the entire depth profile with the inset of the top 20 cm and b) the silt+clay (<63 µm) fraction and three compound classes extracted from the silt+clay for the entire depth profile with the inset of the top 20 cm. For TLE and AA fractions (n=2) and error bars represent the standard error from duplicate measurements. For the <2mm, WEOC, and AI fractions (n=1) and error bars represent analytical error. Error bars are smaller than the marker width where not shown.

4 Discussion

4.1 Variability of compound classes in bulk soils and fractions

We measured radiocarbon content of four distinct soil chemical extracts: water extractable organic carbon (WEOC), total lipid extract (TLE), free amino acids (AA), and the acid insoluble fraction (AI), which had distinct Δ^{14}C values compared to the initial soil fraction each was extracted from (bulk or silt+clay; Fig. 4a and 4b). As expected, Δ^{14}C values of TLE, AA, and AI became more depleted with depth (Fig. 2). More interestingly, the differences between the ^{14}C content of bulk soil and the extracted compounds were not consistent with depth (Fig. 4). This divergence in Δ^{14}C values reflects differences in turnover

https://doi.org/10.5194/egusphere-2023-3125
Preprint. Discussion started: 8 January 2024
© Author(s) 2024. CC BY 4.0 License.

times among compound classes, which can be influenced by the sources of OC to each of these pools and by differences in the stabilization mechanisms protecting those compounds from decay. In this annual grassland, plant inputs should have a greater influence on SOC pools near the surface, which we confirmed with near modern $\Delta^{14}C$ signatures in the 0-10 cm depth for all compound classes and size-fractions (Fig. 3b and 3c). However, at deeper depths, new vegetation inputs should be less readily available, which results in more depleted $\Delta^{14}C$ signatures at depth and could necessitate microbial use and recycling of older SOC.

We found that, averaged across depths, the $\Delta^{14}C$ values of the TLE were more depleted than those of the AA, though both compound classes were more enriched in $\Delta^{14}C$ than the bulk soil or silt+clay that they were extracted from. AAs are the precursors of proteins and found in both plant and microbial biomass. The extracted AAs are hydrolysed proteins can be from both plant material or microbial biomass within the soil sample (Blattmann et al., 2020), so our measurements likely reflect a combination of both plant- and microbially-derived AAs. As in marine studies, we found the AAs to be the youngest compound class fraction (of the TLE and AI) in these soils. The AA pool likely reflects a more actively cycling microbial pool especially at depth, as AA are enriched in nitrogen compounds and likely microbes are both mining and recycling these compounds (Moe, 2013). The divergence from bulk ^{14}C values indicate that even at depth in the soil, the AAs are either continuously replenished from transport of AAs from surface horizons or re-synthesized with relatively ^{14}C enriched sources such as the WEOC.

Based on published data for both soils and marine sediments, we expected the TLE to be older than both the AAs and the bulk soil, however we found that all TLE samples, no matter what fraction we measured, were more ^{14}C enriched than the bulk soil. TLE is composed of a continuum of lipids from plant and microbial materials, ranging from leaf waxes to microbial cell structural components (Angst et al., 2021; Angst et al., 2016), that cycle at different rates and likely interact with mineral surfaces. Previous studies where individual lipid biomarker $\Delta^{14}C$ values were measured in soils on either short chain or long chain fatty acids found that there is a divergence in $\Delta^{14}C$ values between these two pools, with short chain lipids generally having enriched ^{14}C values and long chain lipids having more depleted ^{14}C values (Grant et al., 2022; Van Der Voort et al., 2017). For example, long-chain lipid biomarkers, primarily thought to be plant derived, had consistently older ^{14}C ages than bulk soil (Van Der Voort et al., 2017). Short-chain lipids, which can be microbial or root derived (Rethemeyer et al., 2004), were found to be younger than long-chain lipids throughout the soil profiles and younger than bulk soil at depth (Van Der Voort et al., 2017). However, microbial cell wall lipid biomarkers (glycerol dialkyl glycerol tetraethers, GDGTs) had older ^{14}C ages than bulk soils (Gies et al., 2021). With this consideration, our result of more enriched ^{14}C of the TLE could be an indication of a predominance of short chain lipids and suggested higher abundance of microbially-derived lipids than plant-derived lipids. However further study of specific lipid abundance (e.g., *n*-alkanes, fatty acids) in these soils are necessary, as it is unclear to what degree lipids are older than bulk soils with depth because of preservation of these compounds through mineral association or because of microbial use of aged OC sources for growth.

https://doi.org/10.5194/egusphere-2023-3125
Preprint. Discussion started: 8 January 2024
© Author(s) 2024. CC BY 4.0 License.

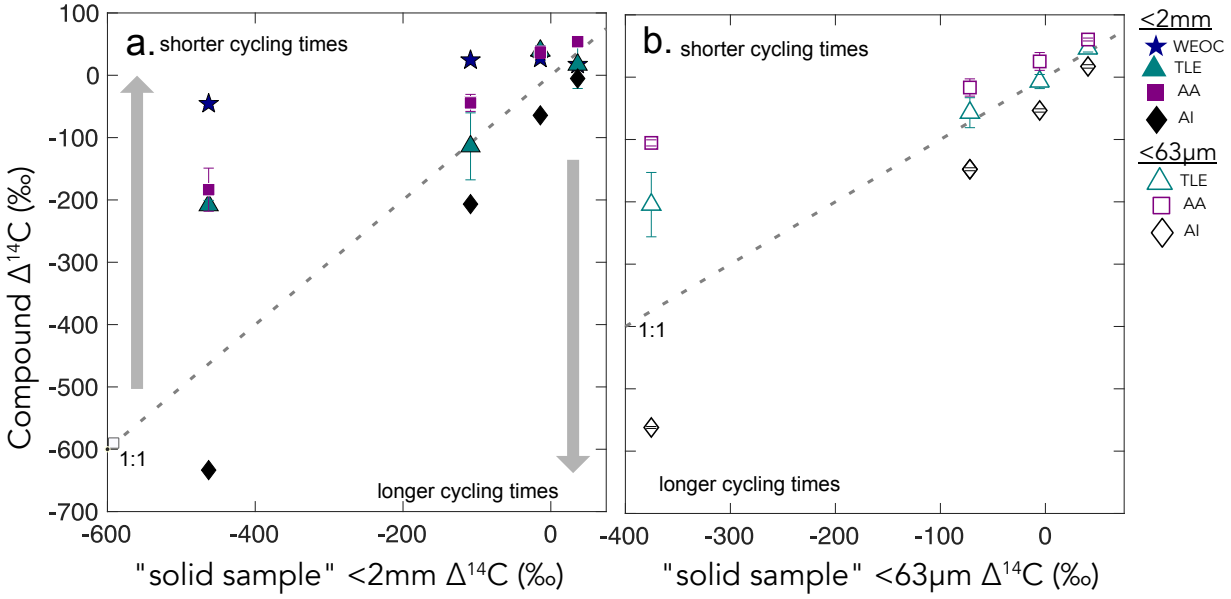

Figure 4. $\Delta^{14}C$ values of the three extracted compound classes (y-axis) compared to the $\Delta^{14}C$ values of the source fraction (x-axis) for a) bulk soil and b) silt+clay. The grey dashed lines show the 1:1 line where bulk sample $\Delta^{14}C$ equals compound class $\Delta^{14}C$. Gray arrows point to regions where data plot above or below the 1:1 line, suggesting that a given compound class has shorter and longer carbon turnover times than bulk soil, respectively.

4.2 Fast cycling OC throughout the depth profile

WEOC (extracted from bulk soils) and POC (<1g mL^{-1} floated off the sand-size fraction) had the most enriched $\Delta^{14}C$ values throughout the soil profile, reflecting a predominance of modern carbon from plant detritus and root exudates to these pools. WEOC fractions can comprise a complex mixture of molecules with different structures (Hagedorn et al., 2004; Bahureksa et al., 2021), which are common only in their ability to be mobilized and dissolved in water. WEOC can mobilize and percolate down the soil profile with sufficient precipitation to allow vertical transport. Both the POC and WEOC fractions supply OC that is readily accessible for microbial degradation and microbial utilization – resulting in the rapid turnover and relatively high $\Delta^{14}C$ values of these two pools (Marin-Spiotta et al., 2011). Occurrence of young OC in deep soils may be driven by microbial uptake of this young and bioavailable DOC or POC. Additionally, we found that the free light-density fractions were depleted in ^{14}C relative to the WEOC and POC (Fig. 5). We suspect this is due to colloidal particles in the FLF, which are not dispersed or dense enough to settle in the SPT.

The study site has a Mediterranean climate, and these soils undergo seasonal wetting and drying cycles. These cycles may intensify in the future (Swain et al., 2018), potentially shifting the composition or amount of OC that percolates down the soil column. When soil is already moist, subsequent rainfall may mobilize both OC and colloidal sized mineral material from reducing conditions which may interact to form stable mineral-OC colloids which can enhance the transport of OC down the

https://doi.org/10.5194/egusphere-2023-3125
Preprint. Discussion started: 8 January 2024
© Author(s) 2024. CC BY 4.0 License.

soil profile and out of the system (Buettner et al., 2014). With prolonged dry periods, water soluble OC may be more susceptible to microbial decomposition or oxidation. This seasonal wetting and drying mechanism likely controls what types of organic matter are transported down the soil profile. Deeper in the soil profile, there is likely greater reactive mineral surface area and less microbial activity, which can enhance carbon stabilization in subsoils (Homyak et al., 2018; Dwivedi et al., 2017; Pries et al., 2023). Further research is needed to understand the effects of seasonal wetting and drying on the behaviour of water-soluble OC in the soil profile.

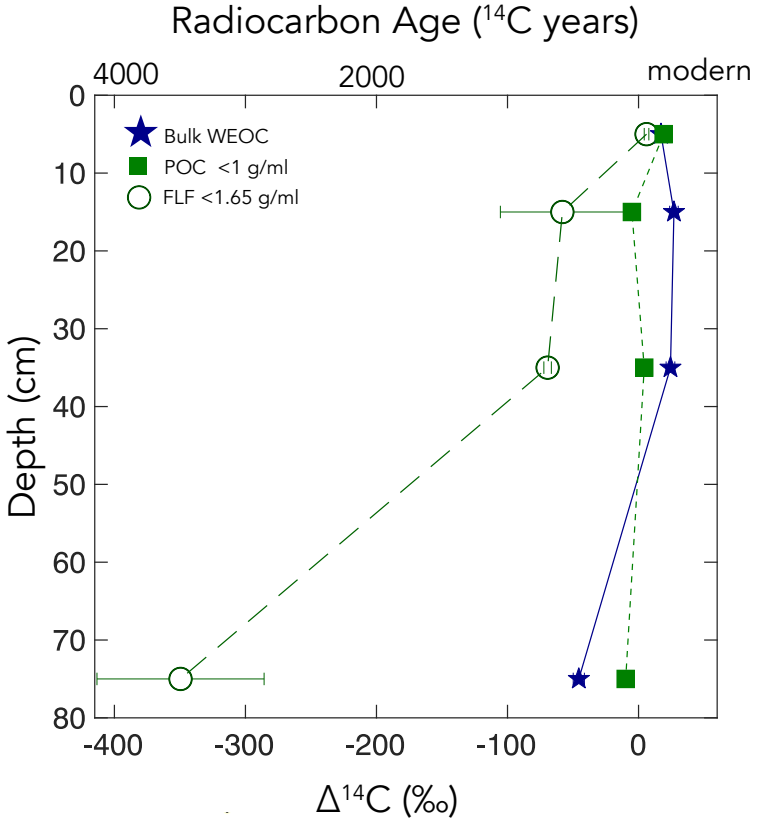

Figure 5: POC (floated from the sand, n = 1), FLF (from bulk soil, n = 3, and error bars indicate standard error on the mean), and WEOC (from bulk soil, n =1). Δ^{14}C values by depth. For POC and WEOC, error bars indicate analytical error are generally smaller than the symbols.

4.3 Compound class Δ^{14}C values in mineral-associated SOC

To investigate the effect of mineral interaction on the Δ^{14}C values or persistence of the TLE, AA, and AI, we measured these extracted compound classes from physical fractions intended to yield approximate mineral-associated carbon pools. We focused primarily on the silt+clay size fraction as the physical fraction that best approximates a mineral-associated OC pool derived from microbially processed plant inputs (Poeplau et al., 2018; Lavallee et al., 2020) and assume that after size

https://doi.org/10.5194/egusphere-2023-3125
Preprint. Discussion started: 8 January 2024
© Author(s) 2024. CC BY 4.0 License.

fractionation most of the free organic matter in the bulk soil was in the sand size fraction. We compared the silt+clay size fraction $\Delta^{14}C$ values to the bulk $\Delta^{14}C$ values to determine if the material extracted from the isolated mineral-associated fractions of the soil had greater OC persistence or if these compounds cycled indiscriminate of mineral association (Fig. 2).

While the TLE from the silt+clay and bulk soil had similar $\Delta^{14}C$ values, the AA from the silt+clay size fraction was enriched in ^{14}C compared to the AA from bulk soil ($r^2 = 0.98$, $p<0.05$). This suggests that AAs cycle faster in the silt+clay mineral pool than in the bulk soils. While mineral surfaces usually are thought to promote stability and persistence of OC, in some soil systems, mineral associations may not be the single defining factor of OC persistence (Rocci et al., 2021) and could have a more nuanced role influencing OC cycling in soils.

Our data suggests there is a continuum of compounds that exist with different ^{14}C values in the mineral-associated pool, because in the silt+clay fraction, the TLE, AA, and AI have significantly different ^{14}C values (Fig. 4b).For instance, the mineral-associated TLE and AA fractions are enriched in ^{14}C relative to the silt+clay fraction, suggesting both are cycling faster than the average mineral associated pool. However, the AI from the silt+clay fraction is cycling slower than solid sample it was extracted from, and when we compare the AI from the bulk soil to the AI from the silt+clay, the AI from the silt+clay is slightly more ^{14}C enriched. This suggests that there is slight ^{14}C enrichment across all different compounds in the silt+clay fraction.

We also compared the TLE extracted from the silt+clay to that extracted from the DF. The mineral-associated fraction is not a uniformly defined pool and is also a consequence of the methodology used to separate the samples (Fig. 6). The DF TLE $\Delta^{14}C$ is significantly older than the silt+clay TLE (Fig. 6b). While the DF TLE could be influenced by methodological differences, such as artifacts from acidic SPT or grinding, it is still more ^{14}C enriched at depth than the TLE of the bulk soil (Fig. 6), which is an indication that at the compound class level, lipids from mineral-associated OC pools still have multiple cycling rates. This is complementary to findings from other studies where ^{14}C values from multiple different lipid biomarkers are divergent from the bulk soils (Gies et al., 2021) and could indicate the necessity of looking at entire compound class pools. These results warrant further investigation into the composition and age-distribution of compounds within mineral associated-OC.

https://doi.org/10.5194/egusphere-2023-3125
Preprint. Discussion started: 8 January 2024
© Author(s) 2024. CC BY 4.0 License.

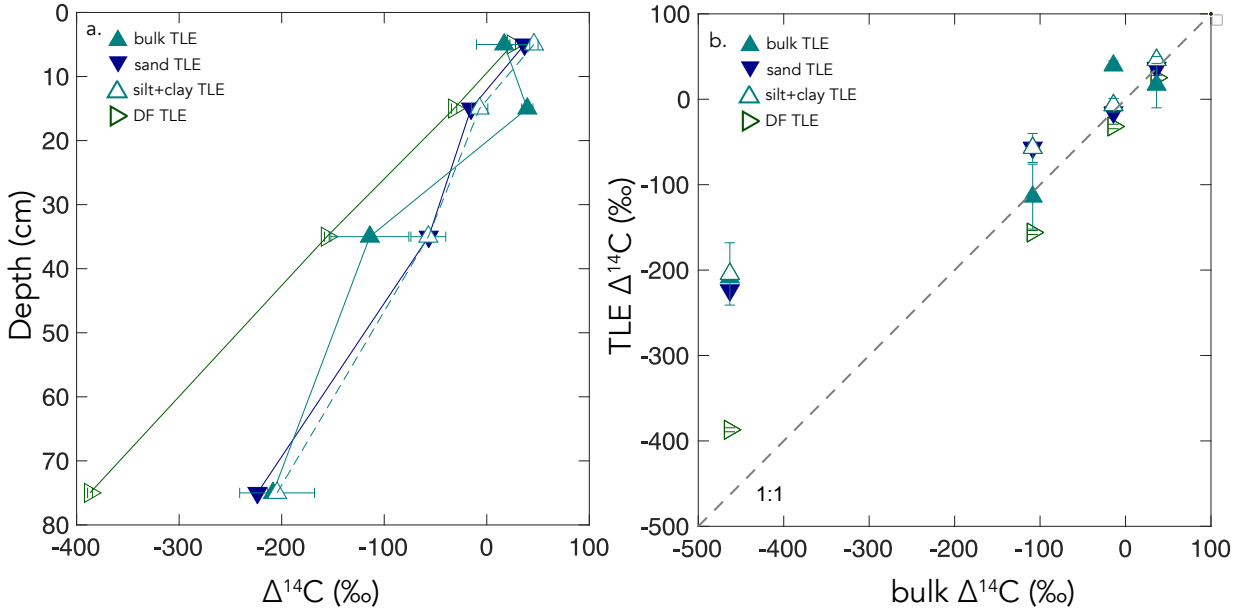

Figure 6: a) $\Delta^{14}C$ versus soil depth measured for TLE extractions from four soil size/density fractions. b) A comparison of the bulk soil $\Delta^{14}C$ values to the TLE from the four size/density fractions.

4.4 Persistent and Petrogenic OC

We found that the most ^{14}C depleted OC fraction measured at each soil depth was the AI (Fig. 3, 4), the residual sample after both the TLE and AA have been extracted (Wang et al., 1998; Wang et al., 2006). The AI fraction was far more depleted relative to the bulk samples (Fig. 2) than in other studies with marine acid-insoluble OC (Wang et al., 2006; Wang and Druffel, 2001). In the marine studies, the ^{14}C is found to be quite variable in age depending on sampling depth or location. The significant depletion of the AI in our soils suggests that these, chemically stable compounds, are not oxidized in soil. Importantly, our AI samples are older than other chemical and physical soil fractions in the soil, which is consistent with the finding that aromatic compounds can be difficult to degrade in in soils (Ukalska-Jaruga et al., 2019).

Since the AI cycles much more slowly than other components of this grassland soil, it is important to understand what structural components make up the AI and where these compounds are sourced from. The chemical structure of the AI fraction has been difficult to characterize. Hwang and Druffel (2003) argued that the AI is a lipid-like portion of the ocean OC. However, in soils, the AI can be composed of a mixture of lipid-like compounds and aromatic compounds (Silveira et al., 2008). In our soil, the ^{13}C-NMR spectra of the AI from 0-10 cm depth show a significant, broad peak in the 100–165 ppm range, indicative aromatics (SI Fig. 3) (Baldock and Preston, 1995; Baldock et al., 1997). While it is possible that some condensed aromatic compounds form during the hydrolysis procedure used to remove AAs, the AI may also contain naturally occurring aromatic compounds that could include pyrogenic or petrogenic OC.

https://doi.org/10.5194/egusphere-2023-3125
Preprint. Discussion started: 8 January 2024
© Author(s) 2024. CC BY 4.0 License.

The parent material of our site is a mixture of sandstone, shale, graywacke, and schist (Foley et al., 2022), so it is possible that some of the OC in our soils is ancient, rock-derived, petrogenic carbon that has been incorporated into the soil profile through pedogenesis progresses (Grant et al., 2023). Comparison of the AI to the rock (>2 mm) fraction shows that the AI is younger than the OC contained in the rock fraction (SI Table 1), with the rock fraction $\Delta^{14}C$ values ranging from -481 to -765‰. To calculate the contribution of OC_{petro} into the AI fraction, we used a binary mixing model with endmembers of OC_{petro} and aged SOC based on the method in Grant et al. (2023). The OC_{petro} ^{14}C endmember was -1000 ‰ and we compared and upper and lower range for the aged SOC ^{14}C values using the TLE and bulk ^{14}C values, respectively, from each depth. In the AI extracted from the silt+clay fraction, the OC_{petro} contribution was 4–5% from 0–10 cm depth and 40–53 % in the 50–100cm depth. In AI extracted from the bulk soil, the OC_{petro} contribution was 0–1 % in the 0–10 cm depth, and 17–44 % in the 50–100 cm depth. Therefore, while the AI fraction likely contains OC_{petro}, it is primarily composed of OC compounds derived from more recent plant and microbial inputs that are highly resistant to acid hydrolysis either because of their chemical structure or their strong associations with minerals.

4.5 Comparison of Fractionated Samples

We focus on the silt+clay fraction as an operationally defined mineral-associated OC pool. Numerous soil physical fractionation schemes have been applied to soils and disparities in methods challenge interpretation and intercomparison of results from different studies using different approaches. We compared our size-based approach to density fractionation of our soils to aid in interpretation and comparability of our findings to other studies. Our silt+clay fraction had higher $\Delta^{14}C$ values than the sand, POC-free sand, and the DF. Our silt+clay fraction may include free organic matter that passed through the 63 μm sieve but that would have floated off the DF during density fractionation. We assume that this small-size free OC is a small fraction of the silt+clay OC as no small fragments of organic matter were visible and because the C:N ratios of the silt+clay fraction are only slightly elevated compared to both the bulk and sand fraction (SI Table S1). For reference, the FLF has high C:N reflecting the high OC content of this fraction (SI Table S1). Rather, the source of ^{14}C-enriched in the silt+clay relative to the POC-free sand and bulk soil may be a result of higher surface area in the silt+clay for association of surface derived OC with minerals.

Additionally, our TLE comparison on different size and density fractions highlights the important influence that method selection has over experimental results. The mineral-associated TLE cycled more rapidly than the bulk soil no matter which "mineral-associated" fraction (the silt+clay or the DF) was chosen. The $\Delta^{14}C$ values of TLE from the bulk, sand, and silt+clay were indistinguishable from one another, possibly because the size fractionation scheme did not effectively separate distinct lipid pools. However, the $\Delta^{14}C$ values of TLE from the DF were significantly more ^{14}C depleted than TLE from the silt+clay size fraction (Fig. 6), suggesting there were older lipids in the DF relative to the silt+clay. However, more depleted ^{14}C values found in the TLE from the DF compared to the silt+clay could have resulted from the DF being exposured to SPT and/or ground after drying and before lipid extraction. It is possible that grinding the DF prior to lipid extraction increased the exposed surface area and resulted in a larger fraction of old SOC or rock-derived OC being incorporated into the TLE than if the DF

https://doi.org/10.5194/egusphere-2023-3125
Preprint. Discussion started: 8 January 2024
© Author(s) 2024. CC BY 4.0 License.

had not been ground. Clearly, the approach used to fractionate soils influences experimental results and must be considered when trying to understand how the persistence of OC changes in different defined soil OC pools.

5 Conclusions and Continued soil radiocarbon compound class characterization

In this study, we characterized a soil carbon profile using compound-class ^{14}C analyses. We found that our extraction methods yielded fractions with ^{14}C signatures distinctly different from the bulk soil from which they were extracted. We found that in this grassland soil, the AA and the TLE fractions cycle more rapidly than the bulk soil throughout the soil profile. At each depth, the AI fraction is the oldest fraction and contains a combination of slowly cycling SOC and ancient petrogenic C. These results show that soil compound classes cycle differently than similar components in marine systems. Our results also show that mineral-associated SOC contains a mixture of carbon compounds with distinctly different ages and sources that drive turnover and persistence. Compound-specific ^{14}C approaches hold promise for improving our understanding of the chemical structure of soil organic carbon, as well as the connection between carbon degradation and preservation in soils. A molecule-resolved understanding of the relationship between compound classes and carbon persistence will also give insight into the fate and turnover time of specific organic biomarkers found in plant residues or the biomass of bacteria, fungi and microfauna. These techniques can also help to determine mechanisms promoting mineral stabilization of soil carbon, especially when combined with soil physical fractionation.

Results from this study highlight that radiocarbon measurements of specific organic compounds and compound classes in soil provide valuable insights into the persistence and decomposition rates of soil organic carbon. To improve our ability to model the future of soil carbon stocks and soil quality in the face of a changing global climate, we need further research that interrogates the composition, radiocarbon content, and cycling rates of soil organic carbon and mechanistically links these rates to physical and chemical drivers.

6 Acknowledgements

This work was performed under the auspices of the U.S. Department of Energy by Lawrence Livermore National Laboratory under Contract DE-AC52-07NA27344 and was supported by the LLNL LDRD Program under Project No. 21-ERD-021. LLNL-JRNL-843138. We acknowledge the traditional, ancestral, unceded territory of the Shóqowa and Hopland People, on which this research was conducted. We thank the staff at the Hopland Research and Extension Center who manage the experiment site and Z Kagely for his assistance in digging the soil pit. Additional support for site access, sample collection, and site characterization data was provided by the U.S. Department of Energy, Office of Biological and Environmental Research, Genomic Sciences Program LLNL 'Microbes Persist' Scientific Focus Area (award #SCW1632).

7 Supplemental Tables/Data Availability

A list of all radiocarbon data, stable carbon, and total OC values with a CAMS tracking number for each of the analyses

https://doi.org/10.5194/egusphere-2023-3125
Preprint. Discussion started: 8 January 2024
© Author(s) 2024. CC BY 4.0 License.

used in this publication.

8 Author Contributions: KJM, KMF, TABB, JP, and KEG conceptualized the study. KJM, KMF, TABB, JP secured funding for the project. KEG designed the method and carried out the extractions with input from KJM, KMF, and TABB. CJL carried out the density separations. MNR carried out the water extractions. JDK and MM ran the NMR experiments. KEG, KJM, KMF interpreted the data. KEG prepared the paper with contributions of all co-authors.

9 Competing interests. The authors declare that they have no conflict of interest.

References

Agnelli, A., Trumbore, S. E., Corti, G., and Ugolini, F. C.: The dynamics of organic matter in rock fragments in soil investigated by 14C dating and measurements of 13C, European Journal of Soil Science, 53, 147-159, https://doi.org/10.1046/j.1365-2389.2002.00432.x, 2002.

Angst, G., Mueller, K. E., Nierop, K. G. J., and Simpson, M. J.: Plant- or microbial-derived? A review on the molecular composition of stabilized soil organic matter, Soil Biology and Biochemistry, 156, 10.1016/j.soilbio.2021.108189, 2021.

Angst, G., John, S., Mueller, C. W., Kögel-Knabner, I., and Rethemeyer, J.: Tracing the sources and spatial distribution of organic carbon in subsoils using a multi-biomarker approach, Scientific Reports, 6, 1-12, 2016.

Bahureksa, W., Tfaily, M. M., Boiteau, R. M., Young, R. B., Logan, M. N., McKenna, A. M., and Borch, T.: Soil Organic Matter Characterization by Fourier Transform Ion Cyclotron Resonance Mass Spectrometry (FTICR MS): A Critical Review of Sample Preparation, Analysis, and Data Interpretation, Environmental Science & Technology, 55, 9637-9656, 10.1021/acs.est.1c01135, 2021.

Baldock, J. A. and Preston, C. M.: Chemistry of Carbon Decomposition Processes in Forests as Revealed by Solid-State Carbon-13 Nuclear Magnetic Resonance, in: Carbon Forms and Functions in Forest Soils, 89-117, https://doi.org/10.2136/1995.carbonforms.c6, 1995.

Baldock, J. A., Oades, J. M., Nelson, P. N., Skene, T. M., Golchin, A., and Clarke, P.: Assessing the extent of decomposition of natural organic materials using solid-state <emph type="7">13</emph>C NMR spectroscopy, Soil Research, 35, 1061-1084, https://doi.org/10.1071/S97004, 1997.

Bartolome, J. W., James Barry, W., Griggs, T., and Hopkinson, P.: 367Valley Grassland, in: Terrestrial Vegetation of California, edited by: Barbour, M., University of California Press, 0, 10.1525/california/9780520249554.003.0014, 2007.

Blattmann, T. M., Montluçon, D. B., Haghipour, N., Ishikawa, N. F., and Eglinton, T. I.: Liquid Chromatographic Isolation of Individual Amino Acids Extracted From Sediments for Radiocarbon Analysis, Frontiers in Marine Science, 7, 10.3389/fmars.2020.00174, 2020.

© Author(s) 2024. CC BY 4.0 License.

Bour, A. L., Walker, B. D., Broek, T. A. B., and McCarthy, M. D.: Radiocarbon Analysis of Individual Amino Acids: Carbon Blank Quantification for a Small-Sample High-Pressure Liquid Chromatography Purification Method, Analytical Chemistry, 88, 3521-3528, 10.1021/acs.analchem.5b03619, 2016.

Broek, T. A. B., Ognibene, T. J., McFarlane, K. J., Moreland, K. C., Brown, T. A., and Bench, G.: Conversion of the LLNL/CAMS 1 MV biomedical AMS system to a semi-automated natural abundance 14C spectrometer: system optimization and performance evaluation, Nuclear Instruments and Methods in Physics Research Section B: Beam Interactions with Materials and Atoms, 499, 124-132, 10.1016/j.nimb.2021.01.022, 2021.

Buettner, S. W., Kramer, M. G., Chadwick, O. A., and Thompson, A.: Mobilization of colloidal carbon during iron reduction in basaltic soils, Geoderma, 221-222, 139-145, https://doi.org/10.1016/j.geoderma.2014.01.012, 2014.

Coppola, A. I., Wiedemeier, D. B., Galy, V., Haghipour, N., Hanke, U. M., Nascimento, G. S., Usman, M., Blattmann, T. M., Reisser, M., Freymond, C. V., Zhao, M., Voss, B., Wacker, L., Schefuß, E., Peucker-Ehrenbrink, B., Abiven, S., Schmidt, M. W. I., and Eglinton, T. I.: Global-scale evidence for the refractory nature of riverine black carbon, Nature Geoscience, 11, 584-588, 10.1038/s41561-018-0159-8, 2018.

De Troyer, I., Amery, F., Van Moorleghem, C., Smolders, E., and Merckx, R.: Tracing the source and fate of dissolved organic matter in soil after incorporation of a 13C labelled residue: A batch incubation study, Soil Biology and Biochemistry, 43, 513-519, https://doi.org/10.1016/j.soilbio.2010.11.016, 2011.

Douglas, P. M. J., Pagani, M., Eglinton, T. I., Brenner, M., Curtis, J. H., Breckenridge, A., and Johnston, K.: A long-term decrease in the persistence of soil carbon caused by ancient Maya land use, Nature Geoscience, 11, 645-649, 10.1038/s41561-018-0192-7, 2018.

Dwivedi, D., Riley, W., Torn, M., Spycher, N., Maggi, F., and Tang, J.: Mineral properties, microbes, transport, and plant-input profiles control vertical distribution and age of soil carbon stocks, Soil Biology and Biochemistry, 107, 244-259, 2017.

Eglinton, T. I., Galy, V. V., Hemingway, J. D., Feng, X., Bao, H., Blattmann, T. M., Dickens, A. F., Gies, H., Giosan, L., Haghipour, N., Hou, P., Lupker, M., McIntyre, C. P., Montlucon, D. B., Peucker-Ehrenbrink, B., Ponton, C., Schefuss, E., Schwab, M. S., Voss, B. M., Wacker, L., Wu, Y., and Zhao, M.: Climate control on terrestrial biospheric carbon turnover, Proc Natl Acad Sci U S A, 118, 10.1073/pnas.2011585118, 2021.

Feng, X., Vonk, J. E., Griffin, C., Zimov, N., Montluçon, D. B., Wacker, L., and Eglinton, T. I.: 14C Variation of Dissolved Lignin in Arctic River Systems, ACS Earth and Space Chemistry, 1, 334-344, 10.1021/acsearthspacechem.7b00055, 2017.

Feng, X., Benitez-Nelson, B. C., Montluçon, D. B., Prahl, F. G., McNichol, A. P., Xu, L., Repeta, D. J., and Eglinton, T. I.: 14C and 13C characteristics of higher plant biomarkers in Washington margin surface sediments, Geochimica et Cosmochimica Acta, 105, 14-30, https://doi.org/10.1016/j.gca.2012.11.034, 2013.

Foley, M. M., Blazewicz, S. J., McFarlane, K. J., Greenlon, A., Hayer, M., Kimbrel, J. A., Koch, B. J., Monsaint-Queeney, V., Morrison, K., Morrissey, E., Hungate, B. A., and Pett-Ridge, J.: Active populations and growth of soil microorganisms are framed by mean annual precipitation in three California annual grasslands, Soil Biology and Biochemistry, 108886, https://doi.org/10.1016/j.soilbio.2022.108886, 2022.

Galy, V., Peucker-Ehrenbrink, B., and Eglinton, T.: Global carbon export from the terrestrial biosphere controlled by erosion, Nature, 521, 204-207, 10.1038/nature14400, 2015.

Galy, V., Beyssac, O., France-Lanord, C., and Eglinton, T.: Recycling of Graphite During Himalayan Erosion: A Geological Stabilization of Carbon in the Crust, Science, 322, 943-945, doi:10.1126/science.1161408, 2008.

© Author(s) 2024. CC BY 4.0 License.

Gaudinski, J. B., Trumbore, S. E., Davidson, E. A., and Zheng, S.: Soil carbon cycling in a temperate forest: radiocarbon-based estimates of residence times, sequestration rates and partitioning of fluxes, Biogeochemistry, 51, 33-69, 10.1023/A:1006301010014, 2000.

Gies, H., Hagedorn, F., Lupker, M., Montluçon, D., Haghipour, N., van der Voort, T. S., and Eglinton, T. I.: Millennial-age glycerol dialkyl glycerol tetraethers (GDGTs) in forested mineral soils: 14C-based evidence for stabilization of microbial necromass, Biogeosciences, 18, 189-205, 10.5194/bg-18-189-2021, 2021.

Gleixner, G.: Soil organic matter dynamics: a biological perspective derived from the use of compound-specific isotopes studies, Ecological Research, 28, 683-695, 2013.

Grant, K. E., Hilton, R. G., and Galy, V. V.: Global patterns of radiocarbon depletion in subsoil linked to rock-derived organic carbon, Geochemical Perspectives Letters, 25, 36-40, https://doi.org/10.7185/geochemlet.2312, 2023.

Grant, K. E., Galy, V. V., Haghipour, N., Eglinton, T. I., and Derry, L. A.: Persistence of old soil carbon under changing climate: The role of mineral-organic matter interactions, Chemical Geology, 587, 10.1016/j.chemgeo.2021.120629, 2022.

Hagedorn, F., Saurer, M., and Blaser, P.: A 13C tracer study to identify the origin of dissolved organic carbon in forested mineral soils, European Journal of Soil Science, 55, 91-100, https://doi.org/10.1046/j.1365-2389.2003.00578.x, 2004.

Hein, C. J., Usman, M., Eglinton, T. I., Haghipour, N., and Galy, V. V.: Millennial-scale hydroclimate control of tropical soil carbon storage, Nature, 581, 63-66, 10.1038/s41586-020-2233-9, 2020.

Homyak, P. M., Blankinship, J. C., Slessarev, E. W., Schaeffer, S. M., Manzoni, S., and Schimel, J. P.: Effects of altered dry season length and plant inputs on soluble soil carbon, Ecology, 99, 2348-2362, https://doi.org/10.1002/ecy.2473, 2018.

Hua, Q., Turnbull, J. C., Santos, G. M., Rakowski, A. Z., Ancapichún, S., De Pol-Holz, R., Hammer, S., Lehman, S. J., Levin, I., Miller, J. B., Palmer, J. G., and Turney, C. S. M.: ATMOSPHERIC RADIOCARBON FOR THE PERIOD 1950–2019, Radiocarbon, 64, 723-745, 10.1017/RDC.2021.95, 2022.

Huang, Y., Bol, R., Harkness, D. D., Ineson, P., and Eglinton, G.: Post-glacial variations in distributions, 13C and 14C contents of aliphatic hydrocarbons and bulk organic matter in three types of British acid upland soils, Organic Geochemistry, 24, 273-287, http://dx.doi.org/10.1016/0146-6380(96)00039-3, 1996.

Hwang, J. and Druffel, E. R. M.: Lipid-Like Material as the Source of the Uncharacterized Organic Carbon in the Ocean?, Science, 299, 881-884, doi:10.1126/science.1078508, 2003.

Ishikawa, N. F., Itahashi, Y., Blattmann, T. M., Takano, Y., Ogawa, N. O., Yamane, M., Yokoyama, Y., Nagata, T., Yoneda, M., Haghipour, N., Eglinton, T. I., and Ohkouchi, N.: Improved Method for Isolation and Purification of Underivatized Amino Acids for Radiocarbon Analysis, Analytical Chemistry, 90, 12035-12041, 10.1021/acs.analchem.8b02693, 2018.

Jia, J., Liu, Z., Haghipour, N., Wacker, L., Zhang, H., Sierra, C. A., Ma, T., Wang, Y., Chen, L., Luo, A., Wang, Z., He, J.-S., Zhao, M., Eglinton, T. I., and Feng, X.: Molecular 14C evidence for contrasting turnover and temperature sensitivity of soil organic matter components, Ecology Letters, 26, 778-788, https://doi.org/10.1111/ele.14204, 2023.

Jobbágy, E. G. and Jackson, R. B.: THE VERTICAL DISTRIBUTION OF SOIL ORGANIC CARBON AND ITS RELATION TO CLIMATE AND VEGETATION, Ecological Applications, 10, 423-436, https://doi.org/10.1890/1051-0761(2000)010[0423:TVDOSO]2.0.CO;2, 2000.

https://doi.org/10.5194/egusphere-2023-3125
Preprint. Discussion started: 8 January 2024
© Author(s) 2024. CC BY 4.0 License.

Keiluweit, M., Bougoure, J. J., Nico, P. S., Pett-Ridge, J., Weber, P. K., and Kleber, M.: Mineral protection of soil carbon counteracted by root exudates, Nature Climate Change, 5, 588-595, 2015.

Kleber, M., Sollins, P., and Sutton, R.: A conceptual model of organo-mineral interactions in soils: self-assembly of organic molecular fragments into zonal structures on mineral surfaces, Biogeochemistry, 85, 9-24, 2007.

Kögel-Knabner, I.: The macromolecular organic composition of plant and microbial residues as inputs to soil organic matter, Soil Biology and Biochemistry, 34, 139-162, https://doi.org/10.1016/S0038-0717(01)00158-4, 2002.

Kotanen, P. M.: Revegetation following Soil Disturbance and Invasion in a Californian Meadow: a 10-year History of Recovery, Biological Invasions, 6, 245-254, 10.1023/B:BINV.0000022145.03215.4f, 2004.

Kuzyakov, Y., Bogomolova, I., and Glaser, B.: Biochar stability in soil: Decomposition during eight years and transformation as assessed by compound-specific 14C analysis, Soil Biology and Biochemistry, 70, 229-236, http://dx.doi.org/10.1016/j.soilbio.2013.12.021, 2014.

Lavallee, J. M., Soong, J. L., and Cotrufo, M. F.: Conceptualizing soil organic matter into particulate and mineral-associated forms to address global change in the 21st century, Global Change Biology, 26, 261-273, https://doi.org/10.1111/gcb.14859, 2020.

Lechleitner, F. A., Baldini, J. U. L., Breitenbach, S. F. M., Fohlmeister, J., McIntyre, C., Goswami, B., Jamieson, R. A., van der Voort, T. S., Prufer, K., Marwan, N., Culleton, B. J., Kennett, D. J., Asmerom, Y., Polyak, V., and Eglinton, T. I.: Hydrological and climatological controls on radiocarbon concentrations in a tropical stalagmite, Geochimica et Cosmochimica Acta, 194, 233-252, https://doi.org/10.1016/j.gca.2016.08.039, 2016.

Lehmann, J. and Kleber, M.: The contentious nature of soil organic matter, Nature, 528, 60-68, 10.1038/nature16069, 2015.

Lehmann, J., Hansel, C. M., Kaiser, C., Kleber, M., Maher, K., Manzoni, S., Nunan, N., Reichstein, M., Schimel, J. P., Torn, M. S., Wieder, W. R., and Kögel-Knabner, I.: Persistence of soil organic carbon caused by functional complexity, Nature Geoscience, 13, 529-534, 10.1038/s41561-020-0612-3, 2020.

Loh, A. N., Bauer, J. E., and Druffel, E. R. M.: Variable ageing and storage of dissolved organic components in the open ocean, Nature, 430, 877-881, 10.1038/nature02780, 2004.

Lützow, M. v., Kögel-Knabner, I., Ekschmitt, K., Matzner, E., Guggenberger, G., Marschner, B., and Flessa, H.: Stabilization of organic matter in temperate soils: mechanisms and their relevance under different soil conditions - a review, European Journal of Soil Science, 57, 426-445, 10.1111/j.1365-2389.2006.00809.x, 2006.

Marin-Spiotta, E., Chadwick, O. A., Kramer, M., and Carbone, M. S.: Carbon delivery to deep mineral horizons in Hawaiian rain forest soils, Journal of Geophysical Research: Biogeosciences, 116, 2011.

McFarlane, K. J., Torn, M. S., Hanson, P. J., Porras, R. C., Swanston, C. W., Callaham, M. A., and Guilderson, T. P.: Comparison of soil organic matter dynamics at five temperate deciduous forests with physical fractionation and radiocarbon measurements, Biogeochemistry, 112, 457-476, 10.1007/s10533-012-9740-1, 2013.

Mikutta, R., Mikutta, C., Kalbitz, K., Scheel, T., Kaiser, K., and Jahn, R.: Biodegradation of forest floor organic matter bound to minerals via different binding mechanisms, Geochimica et Cosmochimica Acta, 71, 2569-2590, 2007.

Moe, L. A.: Amino acids in the rhizosphere: From plants to microbes, American Journal of Botany, 100, 1692-1705, https://doi.org/10.3732/ajb.1300033, 2013.

https://doi.org/10.5194/egusphere-2023-3125
Preprint. Discussion started: 8 January 2024
© Author(s) 2024. CC BY 4.0 License.

Nuccio, E. E., Anderson-Furgeson, J., Estera, K. Y., Pett-Ridge, J., De Valpine, P., Brodie, E. L., and Firestone, M. K.: Climate and edaphic controllers influence rhizosphere community assembly for a wild annual grass, Ecology, 97, 1307-1318, 10.1890/15-0882.1, 2016.

Poeplau, C., Don, A., Six, J., Kaiser, M., Benbi, D., Chenu, C., Cotrufo, M. F., Derrien, D., Gioacchini, P., Grand, S., Gregorich, E., Griepentrog, M., Gunina, A., Haddix, M., Kuzyakov, Y., Kühnel, A., Macdonald, L. M., Soong, J., Trigalet, S., Vermeire, M.-L., Rovira, P., van Wesemael, B., Wiesmeier, M., Yeasmin, S., Yevdokimov, I., and Nieder, R.: Isolating organic carbon fractions with varying turnover rates in temperate agricultural soils – A comprehensive method comparison, Soil Biology and Biochemistry, 125, 10-26, https://doi.org/10.1016/j.soilbio.2018.06.025, 2018.

Pries, C. E. H., Ryals, R., Zhu, B., Min, K., Cooper, A., Goldsmith, S., Pett-Ridge, J., Torn, M., and Berhe, A. A.: The Deep Soil Organic Carbon Response to Global Change, Annual Review of Ecology, Evolution, and Systematics, 54, 375-401, 10.1146/annurev-ecolsys-102320-085332, 2023.

R Core Team: R: A language and environment for statistical computing., R Foundation for Statistical Computing [code], 2019.

Repasch, M., Scheingross, J. S., Hovius, N., Lupker, M., Wittmann, H., Haghipour, N., Gröcke, D. R., Orfeo, O., Eglinton, T. I., and Sachse, D.: Fluvial organic carbon cycling regulated by sediment transit time and mineral protection, Nature Geoscience, 14, 842-848, 10.1038/s41561-021-00845-7, 2021.

Rethemeyer, J., Kramer, C., Gleixner, G., Wiesenberg, G. L. B., Schwark, L., Andersen, N., Nadeau, M.-J., and Grootes, P. M.: Complexity of Soil Organic Matter: AMS 14C Analysis of Soil Lipid Fractions and Individual Compounds, Radiocarbon, 46, 465-473, 10.1017/S0033822200039771, 2004.

Rocci, K. S., Lavallee, J. M., Stewart, C. E., and Cotrufo, M. F.: Soil organic carbon response to global environmental change depends on its distribution between mineral-associated and particulate organic matter: A meta-analysis, Science of The Total Environment, 793, 148569, https://doi.org/10.1016/j.scitotenv.2021.148569, 2021.

Schmidt, M. W., Torn, M. S., Abiven, S., Dittmar, T., Guggenberger, G., Janssens, I. A., Kleber, M., Kögel-Knabner, I., Lehmann, J., and Manning, D. A.: Persistence of soil organic matter as an ecosystem property, Nature, 478, 49-56, 2011.

Shi, Z., Allison, S. D., He, Y., Levine, P. A., Hoyt, A. M., Beem-Miller, J., Zhu, Q., Wieder, W. R., Trumbore, S., and Randerson, J. T.: The age distribution of global soil carbon inferred from radiocarbon measurements, Nature Geoscience, 13, 555-559, 2020.

Sierra, C. A., Müller, M., and Trumbore, S. E.: Modeling radiocarbon dynamics in soils: SoilR version 1.1, Geoscientific Model Development, 7, 1919-1931, 10.5194/gmd-7-1919-2014, 2014.

Silveira, M. L., Comerford, N. B., Reddy, K. R., Cooper, W. T., and El-Rifai, H.: Characterization of soil organic carbon pools by acid hydrolysis, Geoderma, 144, 405-414, https://doi.org/10.1016/j.geoderma.2008.01.002, 2008.

Stoner, S., Trumbore, S. E., González-Pérez, J. A., Schrumpf, M., Sierra, C. A., Hoyt, A. M., Chadwick, O., and Doetterl, S.: Relating mineral–organic matter stabilization mechanisms to carbon quality and age distributions using ramped thermal analysis, Philosophical Transactions of the Royal Society A: Mathematical, Physical and Engineering Sciences, 381, 20230139, doi:10.1098/rsta.2023.0139, 2023.

Stuiver, M. and Polach, H. A.: Discussion Reporting of 14C Data, Radiocarbon, 19, 355-363, 10.1017/s0033822200003672, 1977.

https://doi.org/10.5194/egusphere-2023-3125
Preprint. Discussion started: 8 January 2024
© Author(s) 2024. CC BY 4.0 License.

637 Swain, D. L., Langenbrunner, B., Neelin, J. D., and Hall, A.: Increasing precipitation volatility in twenty-first-century
638 California, Nature Climate Change, 8, 427-433, 10.1038/s41558-018-0140-y, 2018.

639 Torn, M. S., Swanston, C. W., Castanha, C., and Trumbore, S. E.: Storage and Tunover of Organic Matter in Soil, in:
640 Biophysico-Chemical Processes Involving Natural Nonliving Organic Matter in Environmental Systems, edited by: Senesi,
641 N., Xing, B., and Huang, P. M., Wiley-IUPAC series in biopysico-chemical processes in environmental systems, John Wiley
642 & Sons, Inc., Hoboken, New Jersey, 219-272, 2009.

643 Trumbore, S.: Age of Soil Organic Matter and Soil Respiration: Radiocarbon Constraints on Belowground C Dynamics,
644 Ecological Applications - ECOL APPL, 10, 399-411, 10.2307/2641102, 2000.

645 Trumbore, S. E. and Harden, J. W.: Accumulation and turnover of carbon in organic and mineral soils of the BOREAS
646 northern study area, Journal of Geophysical Research: Atmospheres, 102, 28817-28830, 10.1029/97jd02231, 1997.

647 Trumbore, S. E. and Zheng, S.: Comparison of Fractionation Methods for Soil Organic Matter 14C Analysis, Radiocarbon,
648 38, 219-229, 10.1017/s0033822200017598, 1996.

649 Ukalska-Jaruga, A., Smreczak, B., and Klimkowicz-Pawlas, A.: Soil organic matter composition as a factor affecting the
650 accumulation of polycyclic aromatic hydrocarbons, Journal of Soils and Sediments, 19, 1890-1900, 10.1007/s11368-018-
651 2214-x, 2019.

652 van der Voort, T. S., Mannu, U., Hagedorn, F., McIntyre, C., Walthert, L., Schleppi, P., Haghipour, N., and Eglinton, T. I.:
653 Dynamics of deep soil carbon – insights from 14C time series across a climatic gradient, Biogeosciences, 16, 3233-3246,
654 10.5194/bg-16-3233-2019, 2019.

655 van der Voort, T. S., Zell, C. I., Hagedorn, F., Feng, X., McIntyre, C. P., Haghipour, N., Graf Pannatier, E., and Eglinton, T.
656 I.: Diverse Soil Carbon Dynamics Expressed at the Molecular Level, Geophysical Research Letters, 44, 11,840-811,850,
657 10.1002/2017gl076188, 2017.

658 Vogel, C., Mueller, C. W., Höschen, C., Buegger, F., Heister, K., Schulz, S., Schloter, M., and Kögel-Knabner, I.:
659 Submicron structures provide preferential spots for carbon and nitrogen sequestration in soils, Nature Communications, 5,
660 2014.

661 Vogel, J. S., Southon, J. R., Nelson, D. E., and Brown, T. A.: Performance of catalytically condensed carbon for use in
662 accelerator mass spectrometry, Nuclear Instruments and Methods in Physics Research Section B: Beam Interactions with
663 Materials and Atoms, 5, 289-293, https://doi.org/10.1016/0168-583X(84)90529-9, 1984.

664 von Lutzow, M., Kogel-Knabner, I., Ekschmitt, K., Flessa, H., Guggenberger, G., Matzner, E., and Marschner, B.: SOM
665 fractionation methods: Relevance to functional pools and to stabilization mechanisms, Soil Biology and Biochemistry, 39,
666 2183-2207, 2007.

667 Wang, X.-C. and Druffel, E. R. M.: Radiocarbon and stable carbon isotope compositions of organic compound classes in
668 sediments from the NE Pacific and Southern Oceans, Marine Chemistry, 73, 65-81, https://doi.org/10.1016/S0304-
669 4203(00)00090-6, 2001.

670 Wang, X.-C., Callahan, J., and Chen, R. F.: Variability in radiocarbon ages of biochemical compound classes of high
671 molecular weight dissolved organic matter in estuaries, Estuarine, Coastal and Shelf Science, 68, 188-194,
672 10.1016/j.ecss.2006.01.018, 2006.

https://doi.org/10.5194/egusphere-2023-3125
Preprint. Discussion started: 8 January 2024
© Author(s) 2024. CC BY 4.0 License.

673 Wang, X.-C., Druffel, E. R. M., Griffin, S., Lee, C., and Kashgarian, M.: Radiocarbon studies of organic compound classes
674 in plankton and sediment of the northeastern Pacific Ocean, Geochimica et Cosmochimica Acta, 62, 1365-1378,
675 https://doi.org/10.1016/S0016-7037(98)00074-X, 1998.

676

677